NASA CR-54907
Series 7, Issue 22

GPO PRICE $ _____

CFSTI PRICE(S) $ _____

Hard copy (HC) 2.00

Microfiche (MF) .50

ff 653 July 65

QUARTERLY PROGRESS REPORT:

INVESTIGATION OF KILOVOLT ION SPUTTERING

by

HAROLD P. SMITH, JR., F. C. HURLBUT AND T. H. PIGFORD

prepared for

NATIONAL AERONAUTICS AND SPACE ADMINISTRATION

CONTRACT NAS 3-5743

SPACE SCIENCES LABORATORY

UNIVERSITY OF CALIFORNIA, BERKELEY

NASA CR - 54907
Series No. 7, Issue 22

QUARTERLY PROGRESS REPORT:

INVESTIGATION OF KILOVOLT ION SPUTTERING

by

Harold P. Smith, Jr., F. C. Hurlbut, and T. H. Pigford

prepared for

NATIONAL AERONAUTICS AND SPACE ADMINISTRATION

April 30, 1966

CONTRACT NAS 3-5743

Technical Management
Nasa Lewis Research Center
Cleveland, Ohio

Electric Propulsion Office
Mr. J. A. Wolters

SPACE SCIENCES LABORATORY

University of California, Berkeley 94720

TABLE OF CONTENTS

FIGURES

TABLE

I. INTRODUCTION AND SUMMARY

Sputtering or ionic erosion of the accel electrode and focusing structure of the ion rocket engine can be the dominant mechanism limiting long term operation of the engine. Although the field of sputtering has been known since the phenomenon of gas discharge was first observed, no reliable theory to predict the yield, angular distribution, and velocity spectrum has been developed. Furthermore, it has only been within the past few years that experiments have been made under suitably defined conditions. In addition, there has been little work with either cesium or mercury beams so that it is difficult to predict the electrode erosion on the basis of previous data. For these reasons, the Lewis Research Center has sponsored detailed investigation of the sputtering of single crystals of suitable electrode material under cesium and mercury ion beam bombardment where the target parameters such as temperature, angle of incidence, etc., are well known and varied over the range of interest.

The University of California (Berkeley) Space Sciences Laboratory began an investigation of this field early in 1964. This document is submitted as a report of progress in this investigation for the period of time from February through April, 1966.

Apparatus for mercury ion sputtering using radioactive tracer analysis has been completed. An initial experimental run has been successfully completed. Apparatus for cesium ion sputtering has been improved, and ability to analyze the results by electron microprobe of the collector faces has been demonstrated. A detailed experimental investigation of surface roughening during ion implantation is in progress.

Initial results are reported. Measurement of cesium ion sputtering of molybdenum for incident ion variation from 1 to 7.5 KeV and target temperature variation from 77°K to 200°C have been completed. The importance of thermal annealing on incident ion penetration is emphasized. Continued efforts in developing a time-of-flight technique for measurement of the neutral particle velocity spectrum and in developing a method for measurement of surface density through proton induced x-ray techniques are described.

II. MERCURY ION SPUTTERING*

Additional analyses of the mercury ion beam have been completed. The beam composition at the entrance to the magnet chamber under typical operating conditions has been determined magnetically to consist of Hg^+ and Hg^{++} ions only. The ratio of Hg^+/Hg^{++} can be controlled from greater than 200 down to about 10 by varying the arc voltage from 30 to 100 V. As time permits, the possibility of obtaining a Hg^{++} beam of sufficient magnitude to be used for meaningful sputtering will be examined. At the target position, the energy distribution of the Hg^+ beam has been determined by a retarding potential method for an 8.0 KeV beam. For this beam, $\Delta E/E_0$ was approximately 3%. The ion beam profile at the target was investigated for energies of five through ten KeV. It was found that from 70% to greater than 99% of the ion beam hit the target within a radius of three millimeters. At 5 and 6 KeV the collimator intercepted up to 30% of the beam; hence for energies below six KeV a different collimator will be used. During these measurements the source was held at 8 KV and the target assembly floated to cover the given energy range. The hope is that it will be possible to hold the source at 10 KV and the target at -10 KV thereby obtaining Hg^+ ion energies up to 20 KeV.

A trial angular distribution measurement was made using ten KeV Hg^+ ions on a monocrystalline Cu target at 293°K. The target was aligned with the <100> direction parallel to the ion beam. The distribution was determined by the same radioactive tracer technique that was used in the

---

* The work reported in this section was performed by R. G. Musket

sputtering of Cu and Mo by Cs^+. The collector is shown in Figure 1. Figure 2 gives the angular values (θ , Φ , $\Delta\Omega$) for the individual collectors. The relative angular yield and other data are given in Figure 3. It should be noted that those parts of the 2π solid angle not subtended by aluminum foils, where the front foil covers that part of the collector shell not sectioned; the back refers to the foil in plane of target, and the top and bottom complete the 2π enclosure. The ratio of the arrival rate of residual gas to the target removal rate by sputtering can easily be determined (from Figure 3) to be less than .08. Vacuum problems prevented obtaining a smaller value during this measurement. It is expected that this can be improved to at least .02. It should be noted that a concentration of sputtered Cu is in evidence near collector number 56. This spot corresponds to <110> direction in the crystal.

The electron bombardment source has been operated with argon thereby producing a 900 μamp, 3 KeV Ar^+ ion beam at about 2×10^{-5} Torr. This demonstrates the versatility of the source and hence the system as a whole.

It is expected that in the next quarter most of the Hg^+ ion sputtering will be obtained.

III. SURFACE DENSITY MEASUREMENTS*

The surface density of oxygen atoms on an aluminum substrate may be determined by detecting and counting characteristic oxygen x-rays produced by bombardment with a 100 KeV proton beam using a gas proportional counter, coupled with suitable pulse height discriminating and pulse counting equipment.

Due to the low energy of the characteristic oxygen x-rays (500 eV), the proportional counter window must be extremely thin for adequate transmission and yet be able to withstand the necessary proportional counter gas pressure. The minimum gas pressure required is established by requiring that at the maximum counter voltage the gas multiplication be large enough to produce pulse heights for the characteristic oxygen x-rays above the noise level of the pulse amplifying equipment.

In previous reports [2] a technique for preparing thin alumina windows (4000Å) in aluminum foil was described. This type of window assembly was found to withstand approximately 40 Torr gas pressure.

Characteristic oxygen x-rays were produced by bombardment of an anodized aluminum target with the duoplasmatron ion beam. It was found that the pulse heights corresponding to the characteristic oxygen x-rays were less than the noise level of the electronic equipment at the maximum permitted proportional counter pressure of 40 Torr. Consequently it was necessary to decrease the electronic noise level and modify the window assembly for higher gas pressures.

---

* The work reported in this section was performed by R. R. Hart

Several commercial pulse preamplifiers and amplifiers were tested for their low noise characteristics. The best results were obtained with field effect transistor preamplifiers and pulse shaping linear amplifiers. Accordingly, such a system has been ordered and is due to arrive in May.

The counter window assembly was modified so as to permit higher counter gas pressures by anodizing a 1/16 inch thick aluminum plate instead of aluminum foil and then chemically removing the aluminum in the center of the plate leaving an alumina window (~ 4000Å).[3] This modification considerably increased the burst pressure for the window, since the aluminum plate is rigid whereas the aluminum foil is able to flex under pressure.

Further backing for the window was provided by placing a commercially available fine mesh nickel screen (250 lines/inch, 70% transmission) on the window. The screen was firmly held in place by a brass weight. This type of window assembly was found to withstand greater than 100 Torr gas pressure for a 5/16 inch diameter window.

At those higher proportional counter gas pressures and with the low noise pulse amplifying system, it is expected that the oxygen x-ray peak will be well above the electronic noise. This point will be tested next quarter in addition to installing a beam analyzing magnet due to arrive in June and designing a target assembly.

IV. ALUMINUM SPUTTERING*

The experimental arrangement for determination of the angular distribution of sputtered aluminum atoms is now completed and is in the process of being tested for leaks and ion beam transmission.

Extremely high resolution is available using the electron microprobe to scan the collecting cubes to determine the surface density of the sputtered aluminum. The limiting factor in the overall resolution of the measurement is then the solid angle that the target makes with any point on a collector cube. For this reason, a new strong focusing lens system was installed. The beam area on the target will be diminished to an expected diameter of about 1/8 inch. In addition a higher total current is expected which will produce a higher current density than previously realized. A valve to separate the source chamber from the target chamber was installed to allow the source chamber to be sealed off following a sputtering operation. This allows the target chamber to be opened immediately without having to wait for the tungsten tip to cool.

Preliminary checkout runs on the new system will begin shortly and will include the use of an image converter which will visually display on a fluorescent screen the size, shape and orientation of the ion beam.

A great deal of effort has been put into the preparation of the copper collecting cubes and the single crystal aluminum target. For both the sputtering and the electron microprobe analysis a highly polished surface is necessary. It is estimated that to sputter away 100 μgm of Al from a 1/16 inch diameter circle, about 3 microns will be removed.

---

* The work reported in this section was performed by E. H. Hasseltine

A surface with defects less than 1 micron at the very most is necessary then for angular distribution measurements. The electrons from the electron microprobe will penetrate from 1 to 3 microns, and clearly here again the surface must be free of defects down to fractions of a micron or else the electrons and resultant x-rays will be attenuated non-uniformly. The copper cubes were polished mechanically using in successive applications #240, #400, and #600 grit grinding papers. The surfaces were then lapped using a #1400 grit in lapping solution. Diamond polishing paste was then used to take the surfaces down to 6 microns and in some cases 1 micron. A final polishing was performed using a slurry of 0.05 micron alumina particles. The surfaces have no visible defects under 1200 x magnification. The polished cubes have been examined with the electron microprobe to determine residual aluminum on the surface due to the polishing. A slight increase in background counts in the aluminum channel is noted, but the effect will not have a significant effect on the angular measurements.

The aluminum target is a (100) face single crystal grown by a Bridgman process. The crystal as grown was chemically polished using a 12 parts phosphoric, 2 parts sulphuric, 1 part nitric acid solution at 90 - 95^{o}. This was done primarily to remove the oxide layer. The crystal was then mechanically polished in two steps using 14 micron and 1 micron diamond paste. The crystal could not be left in this condition, however, as the mechanical polishing deforms the surface. A surface layer was therefore removed by electropolishing in a 20% perchloric acid in methyl alcohol solution at -50^{o}C. X-ray photographs of the crystal showed that this procedure gives a satisfactory single crystal surface. Once again, a 1200 power microscope could reveal no defects.

The procedure for the use of the electron microprobe appears to be satisfactorily established. The x-ray counts obtained are expected to indicate the relative surface concentrations of aluminum. Normally various correction factors would need to be applied, but for the very thin films being examined here, incident and take off angles will have negligible effect. Fluorescent yield due to excitation of aluminum x-rays by copper x-rays is avoided by keeping the electron beam energy lower than the excitation energy of the copper x-rays. The excitation energy for the copper K series is 9.0 KeV, while for aluminum, the K excitation energy is 1.6 KeV. The L_1 excitation energy for copper is 1.1 KeV, so that it can not excite the aluminum.

V. SPUTTERED ATOM ENERGY SPECTRUM MEASUREMENT*

In order to obtain lower pressures at the target surface and in the mass spectrometer ionizer, a separate chamber has been designed and constructed to house the cesium ion source. Differential vac-ion pumping of this chamber, which is connected to the target chamber by a low conductance collimating slit, should reduce the target chamber pressure by an order of magnitude. In addition, the new chamber provides needed room for a long focal length einzel lens system for focus and transport of the beam to the target surface. Deflection plates are mounted in front of the collimating slit but downstream from the lens assembly.

Progress in testing the ion source optics, chamber, and deflection system has been hampered during the past quarter by needed repair to the ion source. This problem was further compounded by breakage in delivery of the repaired source. The vendor has offered his assurances that the source will be available for full time operation during the next quarter. Assuming this is the case, final testing of the pulsed ion system is expected.

The problems noted in the previous report[4] concerning reduction of the signal to noise ratio resulting from multiplier noise and RF pickup have been successfully solved through use of a charge sensitive pre-amplifier mounted directly on the quadrapole output flange. The pulses now have a rise time shorter than 0.5 μsec. and exceed the noise and

---

* The work reported in this section was performed by M. Kosaki and H. P. Smith, Jr.

pickup by over a factor of ten. Final scaling and counting techniques will be completed during the next quarter. This, in conjunction with an operating ion source, should allow initial measurement of the energy spectrum.

VI. ION IMPLANTATION*

Obtaining meaningful results on the penetration of cesium ions under near-saturation conditions by electrolytic stripping of an irradiated target requires that the implantation process produce as few surface irregularities as possible. To minimize the irregularities noted in our earlier experiments with 35 KeV cesium ions on copper, electrodes capable of sweeping the ion beam sinusoidally across the target at a frequency of 200 cycles/sec have been installed and tested.

During this modification a fracture of the molybdenum tube which provides cesium to the porous tungsten ionizer was repaired. Also, modifications were made to operate the ion source at 20 KeV positive, thereby reducing arcing problems and increasing the current and accelerating-voltage capability of the experiment. The apparatus has been reassembled and successfully operated at 20 KeV and 100 μa output.

A potentiometer circuit for electropolishing aluminum targets has been assembled and operated.

A monocrystalline aluminum target has been bombarded with a 16 μa beam of 10 KeV cesium ions, with the beam swept over a target region of 2 x 4 mm, achieving an irradiation of 0.865×10^{19} ions/cm^2 in 2 hours. Some microscopic surface roughening is still observable, as shown in Figure 4. This photograph indicates sub-micron pits in the outermost region of the irradiated area. Considerably less pitting is observed nearer the center of the target, and these marked differences

---

* The work reported in this section was performed by W. Siekhaus, G. Moreau, and T. H. Pigford

are probably not due to the sinusoidal nature of the deflection beam deflection. The beam current is sufficient to operate at considerably larger deflections, and experiments are now underway to avoid these presently unidentified edge effects by this means. Once a reasonably uniform surface appearance is obtained. the nature of the remaining surface pits will be examined by an electron microscope available through another laboratory. Comparison of surface structure after extensive irradiation of polycrystalline and monocrystalline targets will be made.

Assembly of the electron-bombardment ion source for implantation of radioactive ions has been completed. In preliminary tests a beam of 300 μa to 1 ma has been obtained with argon. Further calibration and operation is hindered by the capability of the vacuum system borrowed for this experiment, and the source is now being transferred to a system with the necessary vacuum capability. Initial tests of the entire source-target system will be carried out with nonradioactive argon and krypton. This apparatus will then be used to extend the range of the implantation experiments so that the effects of lower irradiation upon penetration and the approach towards a saturation distribution can be determined.

VII. CESIUM SPUTTERING OF MOLYBDENUM*

The yield and angular distribution of molybdenum sputtered under normal bombardment of the (100) face has been measured as a function of target temperature ($77^{\circ}K < T < 200^{\circ}C$) and incident ion energy ($1.0 \leq E \leq 7.5$ KeV). The experimental apparatus, procedure, and target preparation have been previously described.[4] The results are shown in Table 1 and the yield S(E) is plotted in Figure 5. These results, which will be discussed in detail in a forthcoming publication, are consistent with a model of sputtering that emphasizes the importance of ion penetration and considers focused collision chains to be of secondary importance. This interpretation is supported by comparison with thermal annealing of radiation damage in molybdenum.[5]

---

* The work reported in this section was performed by J. B. Green, N. T. Olson, and H. P. Smith, Jr.

REFERENCES

1. N. T. Olson and H. P. Smith, Jr., AIAA J. (in press).

2. H. P. Smith, Jr., F. C. Hurlbut, and T. H. Pigford, "Quarterly Progress Report: Investigation of Kilovolt Ion Sputtering," NASA CR-54406, October 31, 1965.

3. U. Hauser and W. Kerler, Rev. Sci. Inst. 29, 380 (1958).

4. H. P. Smith, Jr., F. C. Hurlbut, and T. H. Pigford, "Quarterly Progress Report: Investigation of Kilovolt Ion Sputtering," NASA CR-54906, January 31, 1966.

5. G. H. Kinchin and M. W. Thompson, J. Nucl. Energy 6, 275 (1958).

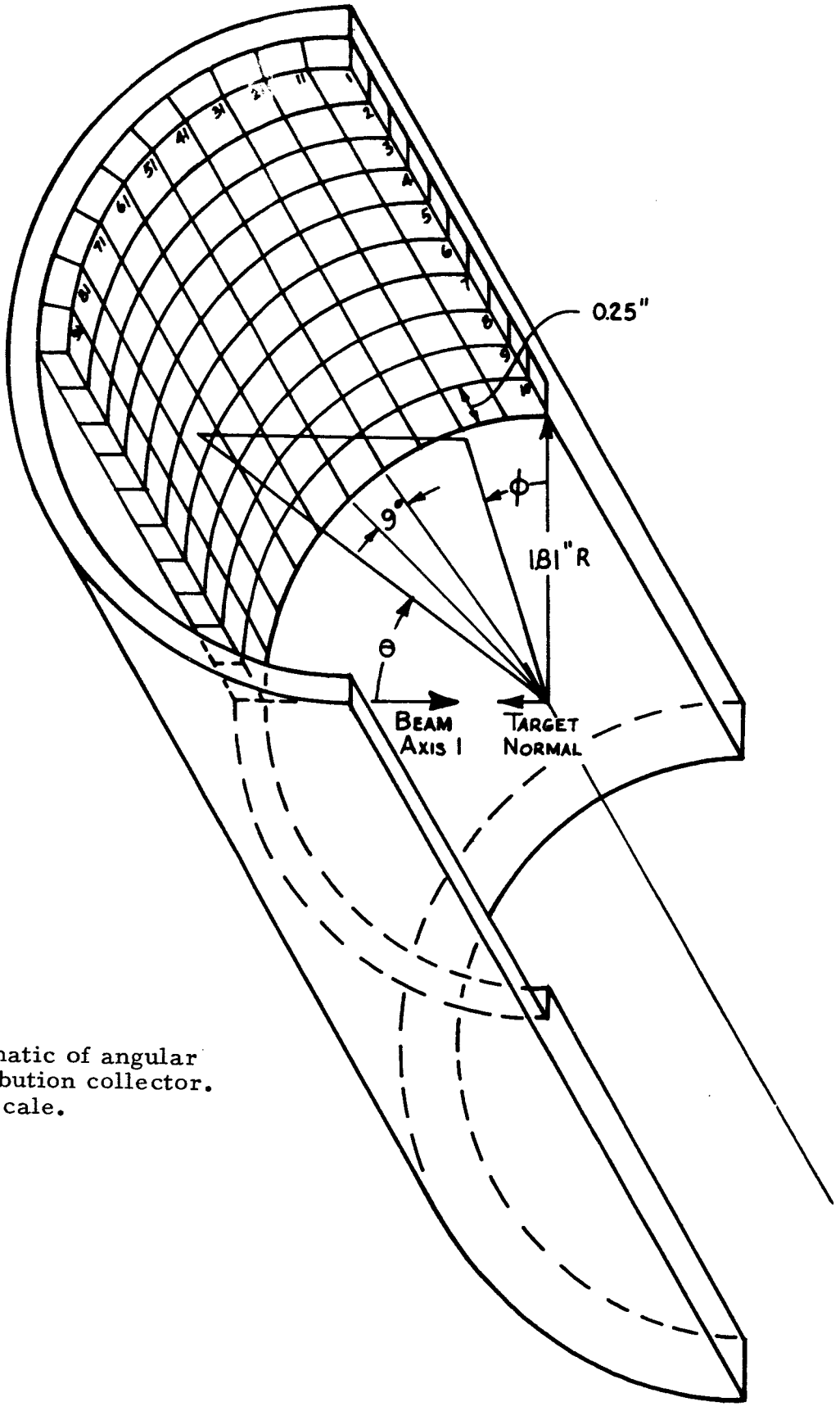

FIGURE 1: Schematic of angular distribution collector. Full scale.

θ(°) Φ(°) ΔΩ(sr)									
52.8 [91] 86.6 .00485 →	53.9 [81] 79.9	56.0 [71] 73.7	58.9 [61] 68.4	62.5 [51] 63.5	66.9 [41] 59.8	71.6 [31] 57.1	76.6 [21] 54.8	81.9 [11] 53.5	87.3 [1] 52.8
49.7 86.2 .00588 →	50.9 78.8	53.1 71.9	56.4 66.0	60.4 60.9	65.0 57.0	70.2 54.0	75.6 51.4	81.3 50.4	87.1 [2] 49.2
46.2 85.7 .00708 →	47.6 77.3	50.1 69.7	53.7 63.2	58.1 57.8	63.2 53.7	68.8 50.6	74.6 48.3	80.7 46.8	86.9 [3] 46.1
42.1 85.0 .00910 →	43.6 75.4	46.5 66.9	50.6 59.8	55.5 54.1	61.0 49.7	67.2 46.5	73.4 44.2	80.0 42.7	86.6 [4] 42.1
37.2 84.1 .0110 →	39.1 72.9	42.5 63.2	47.1 55.6	52.7 49.2	58.8 44.9	65.4 41.8	72.2 39.5	79.3 38.0	86.4 [5] 37.4
32.0 82.8 .0134 →	34.3 69.4	38.2 58.3	43.5 50.0	49.8 43.5	56.5 39.2	63.7 36.2	71.0 34.0	78.6 32.6	86.2 [6] 32.0
26.1 80.8 .0156 →	28.8 64.3	34.7 51.6	39.7 42.8	46.8 36.5	54.1 32.4	62.0 29.6	69.8 27.7	77.9 26.4	85.9 [7] 25.9
18.9 77.2 .0190 →	22.8 56.0	28.8 42.0	36.0 33.5	43.9 27.9	52.0 24.4	60.4 22.1	68.7 20.5	77.2 19.5	87.7 [8] 19.1
12.8 69.3 .0203 →	18.0 41.6	25.3 28.4	33.4 21.7	42.0 17.6	50.5 15.2	59.3 13.7	68.0 12.6	76.8 12.0	85.6 [9] 11.8
5.7 [100] 41.3 .0214 →	14.1 [90] 16.5	22.8 [80] 10.4	31.7 [70] 7.6	40.7 [60] 6.0	49.6 [50] 5.2	58.6 [40] 4.6	67.5 [30] 4.3	76.6 [20] 4.4	85.5 [10] 4.0

FIGURE 2: Angular values for individual collectors

RELATIVE ANGULAR YIELD

$$\left(\frac{\Delta S}{\Delta \Omega} \Big/ \frac{S}{2\pi}\right)$$

DATE: 3/24/66 ION: Hg^+ ENERGY: 10 KeV TARGET: Cu TEMP: 293°K

TOTAL YIELD: 8.62 $\frac{\text{atom}}{\text{ion}}$

91	81	71	61	51	41	31	21	11	1
.910	<.005	.809	.371	.595	.075	.382	.416	.036	.040
.859	.859	.697	.347	.477	.496	.303	.064	.201	2 <.005
.620	.776	.742	.563	.523	.638	.354	.271	.172	3 <.005
1.03	.897	.871	.920	.994	.662	.558	<.005	.005	4 .042
1.50	1.42	1.42	1.67	1.92	1.01	.425	.244	.013	5 .035
1.58	1.54	1.82	2.32	2.86	1.48	.690	.244	.041	6 .034
1.50	1.56	2.11	2.19	2.61	1.51	.622	.229	.122	7 .038
1.40	1.55	1.91	1.91	1.60	.690	.493	.236	.168	8 .040
1.73	1.47	1.42	1.60	1.24	.830	.384	.302	.142	9 .051
100	90	80	70	60	50	40	30	20	10
BEAM	1.57	1.39	1.49	.988	.569	.414	.194	.137	.111

BEAM-TARGET ORIENTATION: BEAM AXIS - Parallel to target norm
TARGET NORMAL - <100>

PERCENT YIELDS: ANGULAR =18.0; FRONT = 75.4; BACK = 2.6; TOP = 1.85; BOTTOM = 2.15.

CURRENT DENSITY: ~ 20 $\mu a/cm^2$; CHAMBER PRESSURE: 2×10^{-7} Torr.

BEAM DIAMETER: ~ .6 cm

FIGURE 3: Relative angular yields

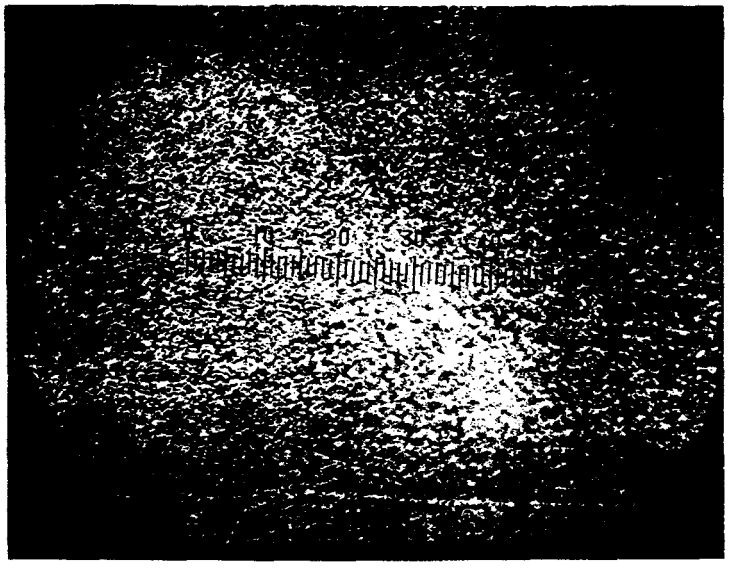

Microphotograph (600 X) of monocrystalline aluminum irradiated with 10 KeV cesium to an average of 0.86 x 10^{19} ions/cm^2. This photograph is taken of the highly pitted area near the edge of the irradiation zone.

FIGURE 4

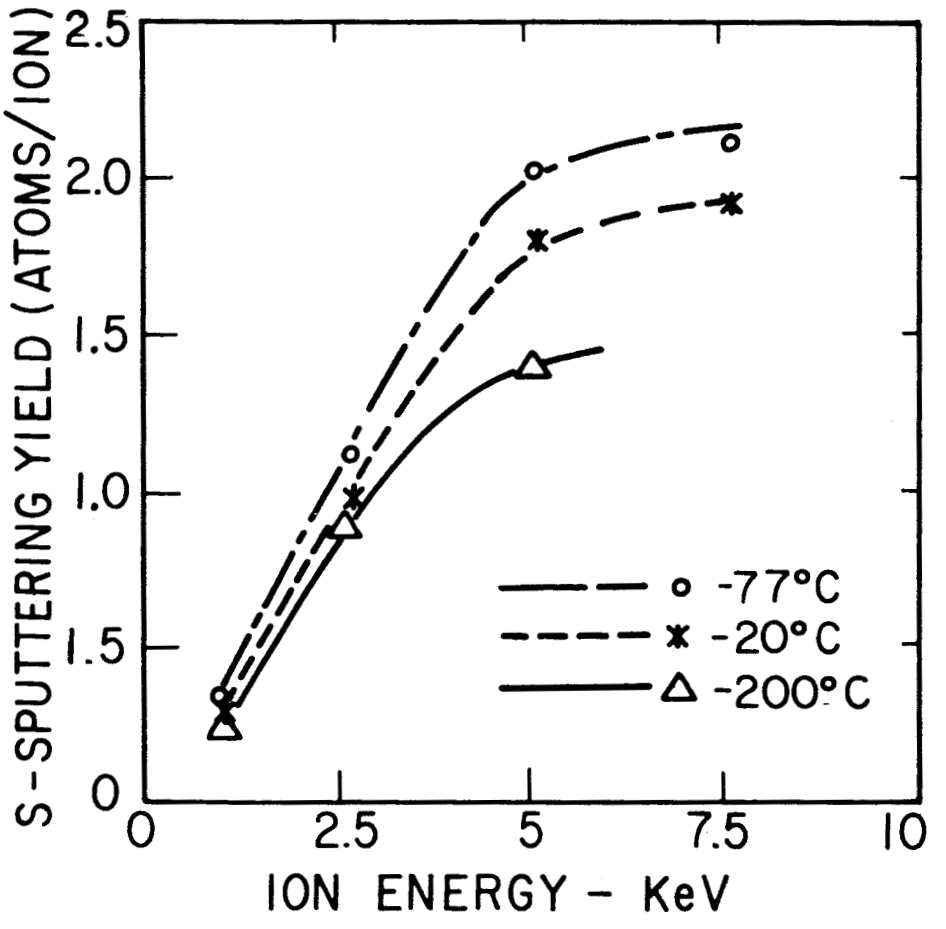

FIGURE 5

Sputtering yield versus incident ion energy as a function of target temperature. Bombardment was normal to the (100) crystallographic face and to the surface.

Ion energy, E(keV)	1.0	2.5	5.0	7.5	2.5	5.0	7.5	5.0
Target temperature, T(°K)	293	293	293	293	77	77	77	493
Yield, S(E, T)	.26	.98	1.78	1.86	1.19	2.05	2.11	1.35
Angular Emission $\frac{2\pi}{S}\frac{dS}{d\Omega}$ Position 1	1.94	2.06	2.03	1.91	2.09	2.03	1.98	2.00
2	2.04	2.11	2.19	2.02	2.23	2.18	2.13	2.18
3	1.91	2.04	2.27	2.08	2.12	2.37	2.31	2.12
4	1.67	1.87	2.17	1.92	2.12	2.39	2.24	1.92
5	1.78	1.80	2.15	1.88	2.13	2.35	2.21	1.90
6	2.08	2.17	2.05	2.02	2.12	1.89	1.93	2.12
7	2.07	2.21	2.03	2.04	2.11	2.00	1.97	2.11
8	2.06	2.18	2.10	1.97	2.15	2.12	2.09	2.10
9	1.93	2.07	2.07	1.91	2.12	2.14	2.07	2.03
10	1.64	1.71	1.78	1.67	1.82	1.89	1.89	1.76
11	2.18	2.30	2.03	2.14	2.06	1.81	1.90	2.15
12	2.21	2.31	2.05	2.11	2.08	1.83	1.86	2.13
13	2.17	2.20	2.05	2.04	2.08	1.88	1.88	2.09
14	1.97	2.06	1.98	1.89	2.06	1.98	1.92	2.00
15	1.86	1.86	1.83	1.73	1.89	1.83	1.93	1.76
16	2.03	2.29	2.14	2.32	2.10	1.95	2.04	2.21
17	2.15	2.31	2.06	2.22	2.07	1.85	1.92	2.18
18	2.20	2.30	2.10	2.16	2.11	1.88	1.91	2.23
19	2.09	2.17	1.99	2.03	2.10	1.93	1.96	2.10
20	1.96	2.00	1.99	1.94	1.99	2.02	1.96	1.94
21	2.05	2.61	2.81	2.98	2.43	2.80	2.92	2.57
22	2.00	2.33	2.22	2.40	2.08	1.97	2.12	2.19
23	2.17	2.30	2.08	2.18	2.08	1.83	1.92	2.17
24	2.13	2.18	2.05	2.08	2.09	1.93	1.96	2.14
25	1.92	2.02	1.97	1.89	2.03	2.03	1.97	1.95
Peak Parameter, N	.23	.45	.51	.68	.12	.20	.23	.57
Coefficient, A	2.18	2.51	2.50	2.58	2.18	2.20	2.20	2.56
Root mean square deviation	.18	.13	.21	.19	.11	.25	.24	.18

Table I.

The yield in atoms/ion and the angular emission normalized to isotropic emission for cesium ion bombardment normal to the (100) face of molybdenum are tabulated as functions of ion energy and target temperature. Position # 21 corresponds to the <100> direction while position #9 corresponds to the <111> direction. The angular data can be represented by $\frac{2\pi}{S}\left(\frac{dS}{d\Omega}\right) \equiv A \cos^N\theta$. The parameters, A and N, are tabulated as well as the root mean square error for each energy and temperature.

Ion energy, E(keV)	1.0	2.5	5.0	7.5	2.5	5.0	7.5	5.0
Target temperature, T(°K)	293	293	293	293	77	77	77	493
Yield, S(E, T)	.26	.98	1.78	1.86	1.19	2.05	2.11	1.35
Angular Emission $\frac{2\pi}{S}\frac{dS}{d\Omega}$ Position								
1	1.94	2.06	2.03	1.91	2.09	2.03	1.98	2.00
2	2.04	2.11	2.19	2.02	2.23	2.18	2.13	2.18
3	1.91	2.04	2.27	2.08	2.12	2.37	2.31	2.12
4	1.67	1.87	2.17	1.92	2.12	2.39	2.24	1.92
5	1.78	1.80	2.15	1.88	2.13	2.35	2.21	1.90
6	2.08	2.17	2.05	2.02	2.12	1.89	1.93	2.12
7	2.07	2.21	2.03	2.04	2.11	2.00	1.97	2.11
8	2.06	2.18	2.10	1.97	2.15	2.12	2.09	2.10
9	1.93	2.07	2.07	1.91	2.12	2.14	2.07	2.03
10	1.64	1.71	1.78	1.67	1.82	1.89	1.89	1.76
11	2.18	2.30	2.03	2.14	2.06	1.81	1.90	2.15
12	2.21	2.31	2.05	2.11	2.08	1.83	1.86	2.13
13	2.17	2.20	2.05	2.04	2.08	1.88	1.88	2.09
14	1.97	2.06	1.98	1.89	2.06	1.98	1.92	2.00
15	1.86	1.86	1.83	1.73	1.89	1.83	1.93	1.76
16	2.03	2.29	2.14	2.32	2.10	1.95	2.04	2.21
17	2.15	2.31	2.06	2.22	2.07	1.85	1.92	2.18
18	2.20	2.30	2.10	2.16	2.11	1.88	1.91	2.23
19	2.09	2.17	1.99	2.03	2.10	1.93	1.96	2.10
20	1.96	2.00	1.99	1.94	1.99	2.02	1.96	1.94
21	2.05	2.61	2.81	2.98	2.43	2.80	2.92	2.57
22	2.00	2.33	2.22	2.40	2.08	1.97	2.12	2.19
23	2.17	2.30	2.08	2.18	2.08	1.83	1.92	2.17
24	2.13	2.18	2.05	2.08	2.09	1.93	1.96	2.14
25	1.92	2.02	1.97	1.89	2.03	2.03	1.97	1.95
Peak Parameter, N	.23	.45	.51	.68	.12	.20	.23	.57
Coefficient, A	2.18	2.51	2.50	2.58	2.18	2.20	2.20	2.56
Root mean square deviation	.18	.13	.21	.19	.11	.25	.24	.18

Table I.

The yield in atoms/ion and the angular emission normalized to isotropic emission for cesium ion bombardment normal to the (100) face of molybdenum are tabulated as functions of ion energy and target temperature. Position # 21 corresponds to the <100> direction while position #9 corresponds to the <111> direction. The angular data can be represented by $\frac{2\pi}{S}\left(\frac{dS}{d\Omega}\right) \equiv A \cos^N\theta$. The parameters, A and N, are tabulated as well as the root mean square error for each energy and temperature.